

EWA PAWLAS-FORYST*, KRZYSZTOF FITZNER**

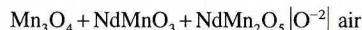
**THERMODYNAMICS OF NdMnO₃ AND NdMn₂O₅ PHASES DETERMINED
BY THE E.M.F. METHOD**

**STABILNOŚĆ TERMODYNAMICZNA FAZ NdMnO₃ I NdMn₂O₅ WYZNACZONA METODĄ PO-
MIARU SIŁY ELEKTROMOTORYCZNEJ OGNIWA**

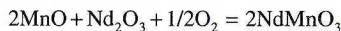
By means of the following solid oxide galvanic cells:



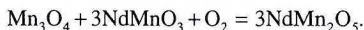
and



the equilibrium oxygen pressure was determined for the reactions:



and



From the determined equilibrium oxygen partial pressure the corresponding Gibbs free energy change for these reactions was derived in the form:

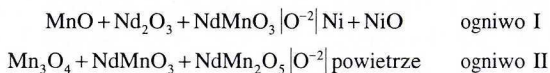
$$\Delta G_{f, \text{NdMnO}_3}^0 = -267241 + 90.34 \cdot T \quad (\text{J})$$

and

$$\Delta G_{f, \text{NdMn}_2\text{O}_5}^0 = -326957 + 223.0 \cdot T \quad (\text{J})$$

Finally, conditions of phase equilibria for the Nd-Mn-O system at fixed pressure and temperature were suggested.

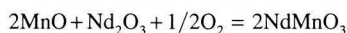
W pracy przedstawiono wyniki badań dotyczące własności termodynamicznych dwóch manganinów neodymu, otrzymane metodą pomiaru SEM następujących ogniwi ze stałym elektrolitem:



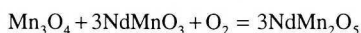
* INSTYTUT METALURGII I INŻYNIERII MATERIAŁOWEJ IM. A. KRUPKOWSKIEGO, PAN, 30-059 KRAKÓW, UL. REYMONTA 25.

** WYDZIAŁ METALI NIEŻELAZNYCH, AKADEMIA GÓRNICZO-HUTNICZA, 30-059 KRAKÓW, AL. MICKIEWICZA 30

oraz wyznaczono równowagowe ciśnienia parcjalne tlenu dla reakcji



i



Z pomiaru tych ciśnień wyznaczono zależności temperaturowe energii swobodnych tworzenia manganinów neodymu NdMnO_3 i NdMn_2O_5 :

$$\Delta G_{f,\text{NdMnO}_3}^0 = -267241 + 90.34 \cdot T \quad (\text{J})$$

i

$$\Delta G_{f,\text{NdMn}_2\text{O}_5}^0 = -326957 + 223.0 \cdot T \quad (\text{J})$$

W oparciu o badania własne oraz dane literaturowe zaproponowano diagramy stabilności faz w układzie Nd-Mn-O w wybranych warunkach ciśnienia tlenu i temperatury.

1. Introduction

One of the most significant innovations in computer industry resulted from a new phenomenon observed for a certain class of inorganic materials. It was found that there are materials whose electrical properties change when they are placed in a magnetic field in such a way that a very small magnetic field causes relatively large change in their resistance at room temperature. This effect, called magneto-resistance, can be in some cases so dramatic that it was called giant magneto-resistance (GMR). GMR effect has been used to boost the storage capacity of computer hard drives up to hundreds of gigabytes. Not surprisingly, when GMR was recently discovered in rare-earth manganates of the type $\text{Ln}_{1-x}\text{A}_x\text{MnO}_3$ (Ln = rare earth, A = divalent cation such as Ca, Sr, Ba), they attracted considerable attention. These metal oxides exhibit perovskite structure which makes them even more interesting. It is this particular structure which in similar metal oxides produced high temperature superconductivity. In this situation one may ask how the substitution of only one component ($\text{Mn} \leftrightarrow \text{Cu}$), which belongs to the same 4th row of the periodic table, can produce such a change in physical properties? No doubt the reason lies in a "genetic code" of the metallic atom: within the oxide structure Mn ($3d^5 4s^2$) with half-filled 3d-shell must produce spatial distribution of electrons entirely different from Cu ($3d^{10} 4s^1$) atom with full 3d-shell. Since the behavior of electrons in the lattice is reflected among others by the materials' electrical conductivity, the conductivity of a large number of simple and perovskite oxide compounds can be compared. Such a comparison made by Torrance *et al.* [1] who used Zaanen *et al.* model [2], shows that oxides can be divided into "metals" and "insulators", and these properties can be described in terms of the relative energies of three electronic energy levels near the Fermi level: fully occupied oxygen 2p states, lowest unoccupied metal orbital and highest occupied 3d or 4d metal states. It is seen that in the group of Mn-compounds only the simple oxide $\beta\text{-MnO}_2$ is "metallic" while in the group of Cu-compounds mixed oxides exhibit high conductivity. Since the position of energy bands is connected with the structure it is perhaps interesting to analyse and

compare compounds and structures formed in respective Cu-*Ln*-O and Mn-*Ln*-O ternary systems.

In general in Cu-systems one can encounter three different types of structures: *T*, *T'* and *T** characteristic for the phase having Ln_2CuO_4 stoichiometry. They differ due to different coordination number of oxygen atoms around copper atoms. The phase with the greatest lanthanide cation La_2CuO_4 exhibits K_2NiF_4 type of structure i.e. *T*. With decreasing cation size (from Pr to Gd) the phase changes the structure into Nd_2CuO_4 , i.e. *T'*. The structure of *T** type may appear if another type of cation (e.g. Sr^{+2}) is introduced into this lattice. Changing the external condition of temperature and pressure one structure can be transformed into the other. Arjomand and Machin [3] showed that under 39.2 MPa and at 1073K $LaCuO_3$ phase can be formed which judging from its stoichiometry should possess Cu^{+3} cations in the lattice. For cations smaller than Gd^{+3} the structure changes and a new phase of $Ln_2Cu_2O_5$ stoichiometry appears in the system. However, Okada et al. [4] showed that this structure can be converted back into *T'* - type under the pressure of 6 MPa and at 1223 K for elements $Ln = Y, Dy, Ho$ and Er . In turn, under lowered oxygen pressure a new phase of $CuFeO_2$ (delafossite) type may appear in the system for elements like $Ln = La, Pr, Nd, Sm, Eu$. Depending on external conditions their mutual relations can be schematically predicted as shown in Fig.1.

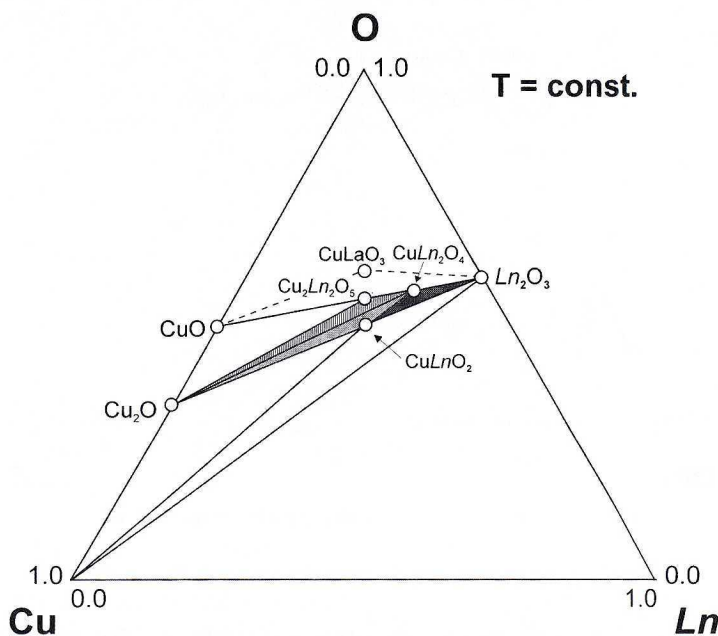


Fig. 1 Schematic ternary diagram for the system *Ln*-Cu-O

Similar analysis conducted for Mn-compounds showed that three different types of ternary oxides may exist. The following types of phases: $LnMnO_3$, $LnMn_2O_5$ and Ln_2MnO_4 were reported. The existence of the Ln_2MnO_4 phase, with tetragonal structure,

was unequivocally confirmed only in Mn-La-O system [5]. Phases of $LnMn_2O_5$ -type seem to be orthorhombic of perovskite type. This was shown experimentally for phases with holmium and dysprosium [6, 7], though the preparation of single crystals by the flux method [7] suggests that all lanthanide phases of this type may exist in the orthorhombic structure.

Phases of $LnMnO_3$ -type were obtained for all rare earth elements. They exist in two types of structural modifications: orthorhombic for elements from La to Dy, and hexagonal based on the ilmenite type for elements from Ho to Lu. [8,9]. The hexagonal structure under high pressure of 4.2–4.5 GPa and at elevated temperatures 950–1123 K can be transformed into perovskite-type structure [10]. Moreover, depending on temperature and oxygen partial pressure, oxygen nonstoichiometry in these compounds may vary from oxygen deficient to oxygen excess. A schematic representation of possible phase equilibria in Ln -Mn-O systems is depicted in Fig. 2

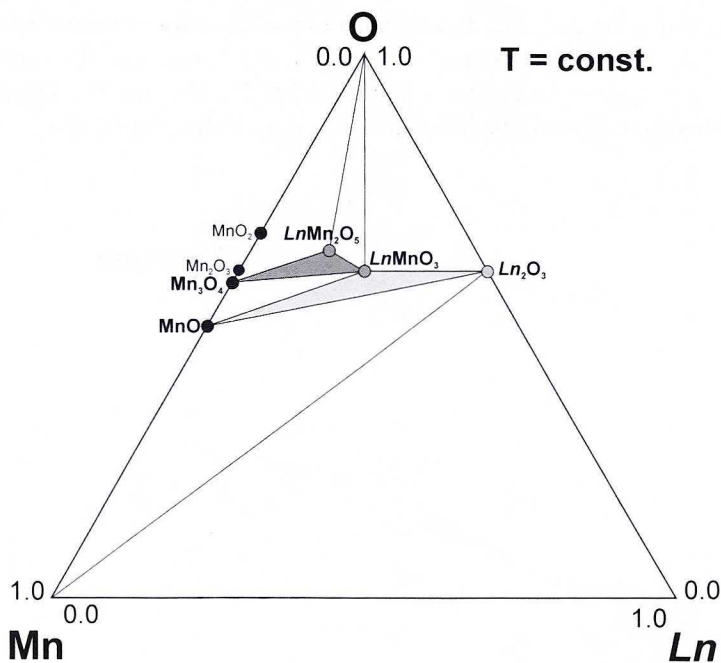


Fig. 2. Schematic ternary diagram for the system Ln -Mn-O

Since the precise knowledge of phase equilibria and thermodynamic stability of respective oxide phases in terms of temperature and oxygen potential is required to define their processing conditions, it is not surprising that attempts are being made to enlarge this kind of information. In a series of papers we reported new data on oxide phases stability obtained in this laboratory for Cu- compounds [11–18]. Using similar experimental technique we intend to investigate a series of Mn-phases starting from neodymium compounds.

2. Experimental

Materials

Pure oxides of Nd_2O_3 (99.9% – BDH Chemical Ltd), MnO (99.9%), Mn_2O_3 and Mn_3O_4 (both prepared by heating of MnO_2 -pure under proper conditions) were used as starting materials to prepare respective phases. At first, Nd_2O_3 was dried at 1273K in air for 24 hours and Mn_2O_3 was calcined at 1023K in the air. Next, an equimolar mixture of Nd_2O_3 and Mn_2O_3 was prepared, pressed into pellets and fired at 1273K in the atmosphere of pure argon for 72 hours. All the samples were quenched very quickly to room temperature in the atmosphere in which they had been fired. Next, the pellets were reground in an agate mortar, pressed once more and heated at 1620 K for 6 hours in the induction furnace also in argon atmosphere but at lower pressure. Phase identification was made by XRD analysis (Philips type PW 1710) and it showed that the material consisted of NdMnO_3 phase only.

The high purity argon gas 99.998% (AGA gas – 4.8) was used to provide an inert gas atmosphere for the synthesis of electrodes, and was additionally deoxidized by passing through copper shavings at 723 K and then through silica gel and anhydrous $\text{Mg}(\text{ClO}_4)_2$.

We tried to obtain the NdMn_2O_5 compound using as substrates previously prepared compounds: NdMnO_3 , Mn_2O_3 and Mn_3O_4 . The equimolar mixtures of NdMnO_3 - Mn_2O_3 and NdMnO_3 - Mn_3O_4 in the form of pressed pellets were placed in the platinum boat inside the quartz tube. The samples were heated at 1223 K for 132 hours in pure oxygen flowing through the system. Then, the samples were cooled quickly by pulling out the Pt boat into furnace cold zone which was cooled by the water jacket. The X-ray powder analysis showed that NdMn_2O_5 was the main product of the reaction, but in the first case the traces of Mn_2O_3 were found. In the second case Mn_3O_4 and NdMnO_3 were present besides of NdMn_2O_5 . We assumed that this product of the synthesis may be used as the electrode ready for the EMF experiments.

Technique

We used the galvanic cell with Ca-stabilized ZrO_2 as solid electrolyte to measure the oxygen pressure at dissociation of the phases NdMnO_3 and NdMn_2O_5 . Two types of e.m.f. cells were used in our experiments and they are shown in Figures 3 and 4. The first cell I (Fig. 3) was applied to the e.m.f. measurements with NdMnO_3 + Nd_2O_3 + MnO phases mixture as the working electrode, and the second one was used to determine the e.m.f. produced by the NdMn_2O_5 + NdMnO_3 + Mn_3O_4 working electrode (Fig. 4).

In the first case the reference electrode was the mixture of Ni + NiO in molar ratio 1.5 : 1. The investigated electrode contained the mixture with the molar ratio 2 : 2.5 : 1. The working electrode and reference electrode were placed in a crucible made of alumina, sealed with high temperature cement and placed in closed one end quartz tube. Before the experiment the whole system was flushed with pure argon. Then, the

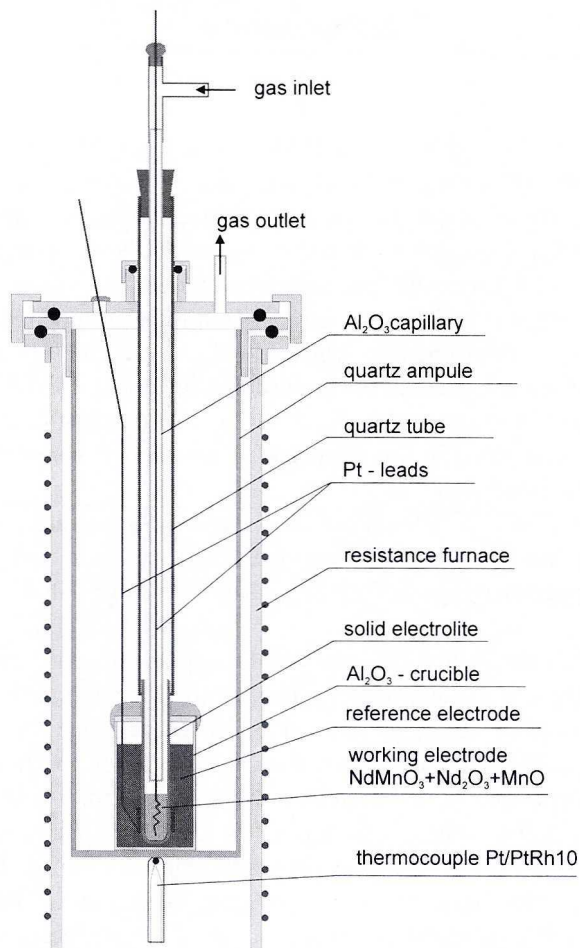


Fig. 3. Schematic diagram of the apparatus used for the emf measurements of cell I

temperature was raised and the cell was working under argon atmosphere. The temperature of the furnace was controlled by Eurotherm temperature controller and e.m.f. was measured with high resistance multimeter Keithley 2000. The course of the experiment (e.m.f. vs. time necessary to reach the equilibrium by the system) was recorded by a computer. The cell was working for about 2 weeks and the measurements were taken at increasing and decreasing temperature.

In the second case the reference electrode was the air (Fig. 4). The working electrode consisted of a mixture of NdMn_2O_5 , NdMnO_3 and Mn_3O_4 , and it was placed inside the tube. Before the experiment the tube was flushed with argon and the flow of argon was maintained during measurements. The e.m.f. measurements were taken in the same way as described before. The whole experimental run took about two weeks.

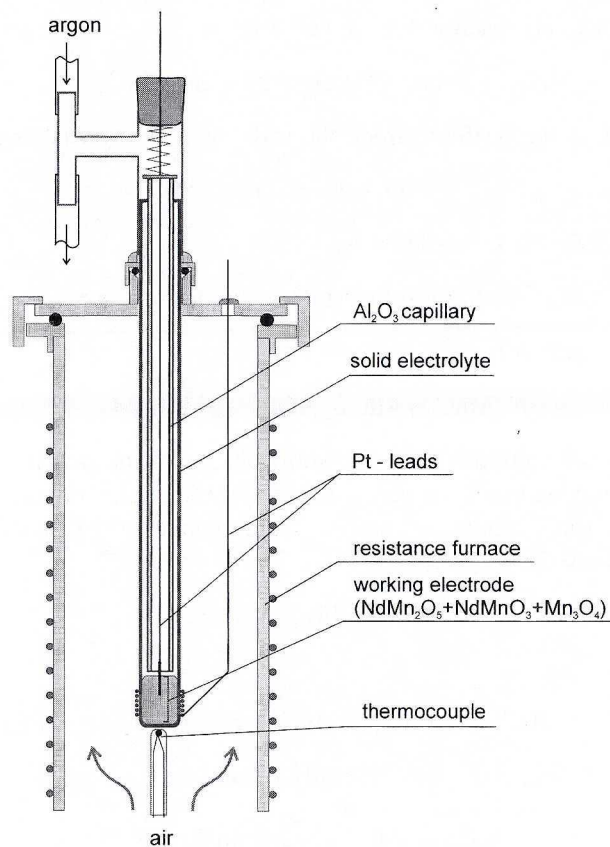


Fig. 4. Schematic diagram of the apparatus used for the emf measurements of cell II

Principles

The following electrochemical cells were assembled:



and



The cells are written in such a way that the right-hand electrodes are positive.

For galvanic cell I electrode reactions are

– at the RHS electrode:



– at the LHS electrode:



Consequently, the net cell reaction for the cell I is:



For galvanic cell II, at the RHS electrode the following reaction takes place:



while at the LHS electrode the reaction is:



The overall cell II reaction is:



Neglecting mutual solubility between solid phases in the investigated temperature range (all solid components of the reaction remain essentially in their standard states) one obtains for the spontaneous cell reactions the change in Gibbs free energy from the following relationship:

$$\Delta G^{\text{I}} = -2FE_{(\text{I})} = \Delta G_{(3)}^0 \quad (7)$$

for the cell I, and

$$\Delta G^{\text{II}} = -4FE_{(\text{II})} = \Delta G_{(6)}^0 - RT \cdot \ln(0.21) \quad (8)$$

for the cell II, from which $\Delta G_{(6)}^0$ can be easily obtained:

$$\Delta G_{(6)}^0 = -4FE_{(\text{II})} + RT \cdot \ln(0.21). \quad (9)$$

Next, combining $\Delta G_{(3)}^0$ with Gibbs free energy change of NiO formation one can derive Gibbs energy of formation of NdMnO₃ according to the reaction:



3. Results

The variations of the EMF's with temperature determined for the investigated systems are shown in Figures 5 and 6. Cells produced reproducible EMF values for more than one week. The corresponding linear relations between EMF and temperature were obtained by the least-squares fit, and have the following form:

$$E_{\text{I}} (\text{mV}) = 173.1 - 0.028 \cdot T / \text{K} \quad (11)$$

$$E_{\text{II}} (\text{mV}) = 846.4 - 0.611 \cdot T / \text{K}. \quad (12)$$

Respective ΔG^0 changes were calculated from our EMF data and are as follows:

$$\Delta G_{(3)}^0 (\text{J}) = -33433 + 5.40 \cdot T / \text{K} \quad (13)$$

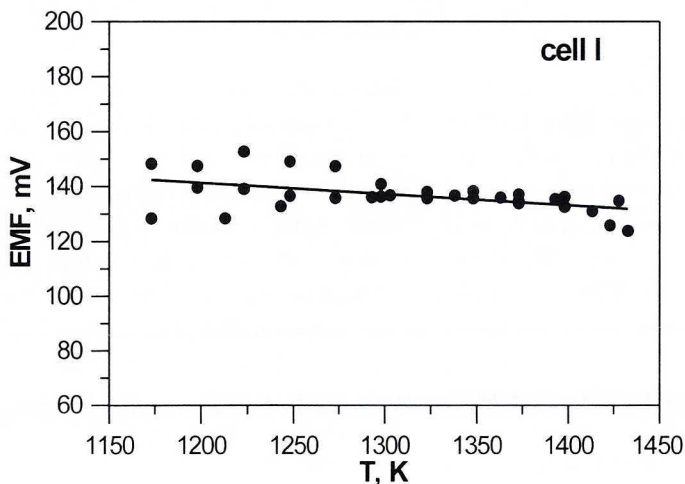


Fig. 5. The emf vs. T plot for cell I

which after addition of $\Delta G_{f, \text{NiO}}^0$, (we accepted this value obtained from e.m.f. measurements after Charette and Flengas [19]), yields the Gibbs free energy change of the reaction (10):

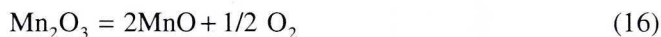
$$\Delta G_{(10)}^0 (\text{J}) = -267241 + 90.34 \cdot T / \text{K} \quad (14)$$

and also

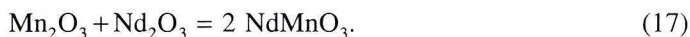
$$\Delta G_{(6)}^0 (\text{J}) = -326957 + 223.0 \cdot T / \text{K} \quad (15)$$

which was obtained directly from eq. 9 assuming $p_{\text{O}_2} = 0.21$ atm at the air reference electrode.

When reaction (10) is combined with the reaction:



the reaction of formation of neodymium manganate NdMnO_3 from respective oxides is obtained:



Thus, combining Gibbs energy changes obtained in this study for the reaction (10) with thermodynamic properties of manganomanganic oxide Mn_3O_4 and manganese sesquioxide Mn_2O_3 determined with high-temperature galvanic cells by Schaefer [20], the Gibbs free energy of formation of NdMnO_3 phase from respective oxides for the reaction;



was derived in the following form:

$$\Delta G_{\text{oxides}}^0 (\text{J}) = -39790 - 8.27 \cdot T / \text{K}. \quad (19)$$

4. Discussion

The thermodynamic stability of NdMnO_3 and NdMn_2O_5 phases was determined in the temperature range from 1000 to 1300 K. Galvanic cells with solid oxide electrolyte were used to determine equilibrium oxygen partial pressure as a function of temperature for respective three-phase equilibria. The cells worked reversibly over a period of about one week which was visible from repeatable e.m.f.'s during temperature cycling up and down. No sign of side reactions was observed during the course of experiments. Examinations of the Pt wire which was in contact with the working electrode after experiments did not show signs of reaction between Mn and platinum. Also, additional experiments with Nd_2O_3 – solid electrolyte equilibration at 1273 K did not show signs of the exchange reaction between these oxides. Thus, one may assume that if there are side reactions in the cell they may take place only at the temperature higher than 1300 K since at lower temperature they are negligible.

The thermodynamic stability of NdMnO_3 was determined by Cherepanov *et al.* [21]. Atsumi *et al.* [22], Kamegashira *et al.* [23], and recently by Jacob *et al.* [24]. In three studies (ref. 21, 22 and 24) the electrochemical technique was applied. Kamegashira *et al.* used isothermal electrical conductivity to detect the decomposition of the phase. Respective Gibbs free energy changes are shown and compared with our values in Fig. 7. It is seen that all e.m.f. results are close to one another while the Gibbs energies of formation obtained from conductivity measurements are less negative. Calculated Gibbs energy change for the reaction of formation of NdMnO_3 from oxides given by eq. (19) is almost identical with that reported by Jacob *et al.* [24].

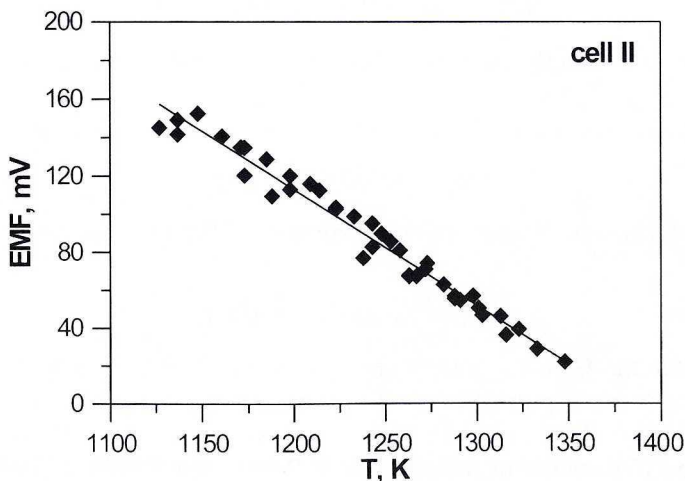


Fig. 6. The emf vs. T plot for cell II

As far as the stability of NdMn_2O_5 compound is concerned two different experimental techniques were used to derive respective Gibbs free energy changes. Cherepanov *et al.* [21] and Jacob *et al.* [24] used e.m.f. measurements while Satoh *et al.* [25]

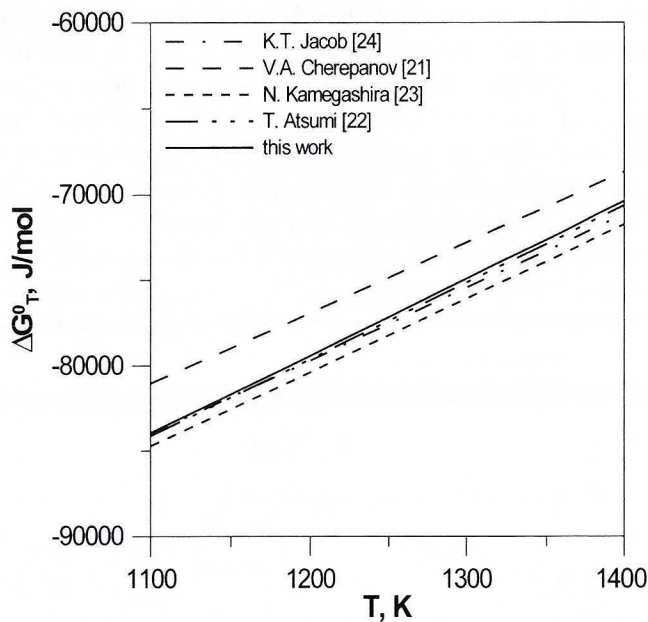


Fig. 7. Comparison of Gibbs energy of NdMnO_3 obtained in this study with data reported in literature

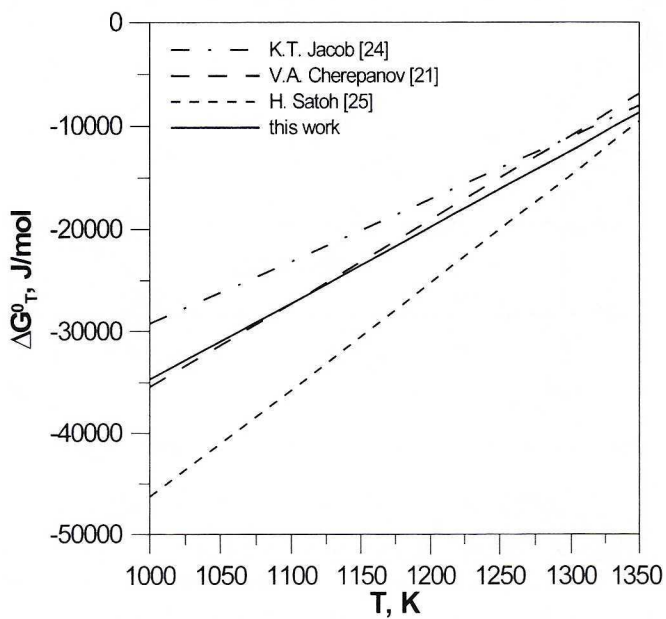


Fig. 8. The plot of Gibbs energy of NdMn_2O_5 formation reaction vs. temperature in the range 1000–1350 K

applied thermogravimetric technique. Gibbs free energy values derived from different studies for the formation of NdMn_2O_5 are compared in Fig. 8. Results are close to one another, though it is obvious that thermogravimetry produced different temperature dependence than e.m.f studies. Due to the particular cell construction with three electrodes Jacob *et al.* probably managed to avoid polarization problems and it seems that temperature dependence given in their study is most precise.

Using the results of this study the oxygen potential diagram for the system Nd-Mn-O was derived for chosen temperature 1273 K and is shown in Fig. 9. The composition variable ξ is the molar fraction $n_{\text{Mn}}/(n_{\text{Mn}} + n_{\text{Nd}})$. The equilibria at a very low oxygen potential are not shown. Also phase relations at constant pressure $p_{\text{O}_2} = 2.1 \cdot 10^4$ Pa as a function of temperature were computed and are shown in Fig. 10. Diagrams show

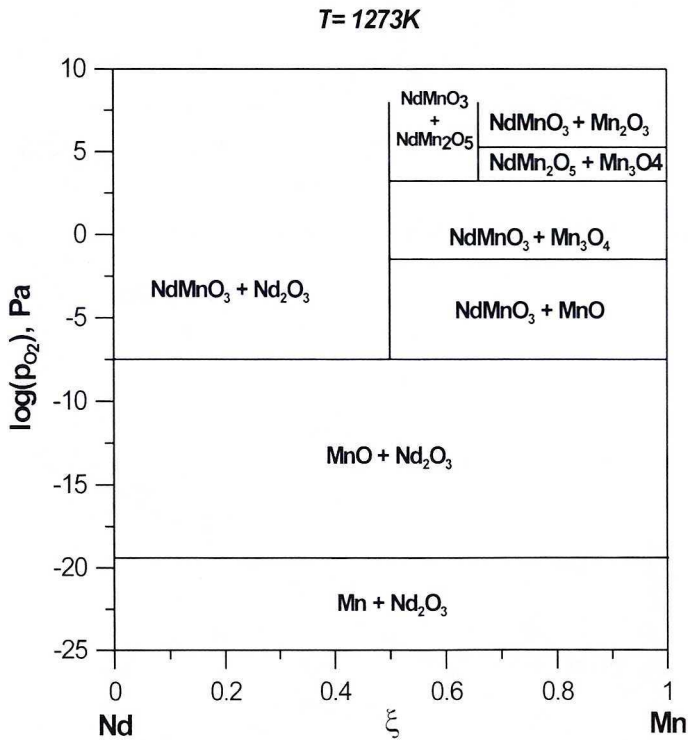


Fig. 9. Phase diagram of the Nd - Mn - O system at constant temperature 1273 K

clearly how stability of various phases may change with the change of external conditions. Similar diagrams can be easily calculated under different conditions described by T and p_{O_2} variables. Since the synthesis of the chosen phase is usually conducted under fixed oxygen pressure and temperature, this type of diagrams is very useful in establishing proper conditions for the preparation of the chosen compound.

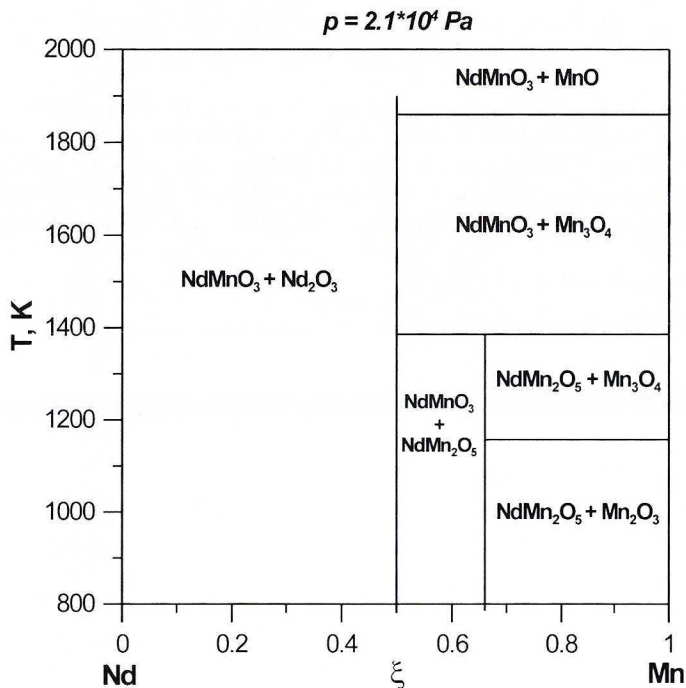


Fig. 10. Phase diagram the Nd – Mn – O system at constant oxygen partial pressure $2 \cdot 10^4 \text{ Pa}$ (0.21 atm)

REFERENCES

- [1] J.B. Torrance, P. Lacorrou, Ch. Asavaroenchai, R.M. Metzger, *J. Solid State Chem.* **90**, 168 (1991).
- [2] J. Zaanen, G.A. Sawatzky, J.W. Allen, *Phys. Rev. Lett.* **55**, 418 (1985).
- [3] M. Arjomand, D.J. Machin, *J. Chem. Soc. Dalton Trans.* 1061 (1975)
- [4] H. Okada, M. Takono, Y. Takeda, *Physica C* **C166**, 111 (1990).
- [5] M.L. Borlera, F. Abbatista, *J. Les-Common Met.* **92**, 55 (1983).
- [6] E.F. Bertaut, G. Buisson, *Bull. Soc. Chim. Franc.* 1132 (1965).
- [7] B.M. Wanklyn, *J. Mater. Sci.* **7**, 813 (1973).
- [8] H.L. Yakel, W.D. Koehler, E.F. Bertaut, F. Forrot, *Acta Crystal.* **116**, 957 (1963).
- [9] K. Kamata, T. Nakajima, T. Nakamura, *Mater. Res. Bull.* **14**, 1007 (1979).
- [10] A. Waintal, J. Chenovas, *Mater. Res. Bull.* **2**, 819 (1967).
- [11] K. Fitzner, *Thermochim. Acta* **171**, 123 (1990).
- [12] W. Przybyło, K. Fitzner, *Arch. Met.* **2**, 141 (1996).
- [13] W. Przybyło, K. Fitzner, *Thermochim. Acta* **264**, 113 (1995).
- [14] M. Kopyto, K. Fitzner, *J. Materials Sci.* **31**, 2797 (1996).
- [15] M. Kopyto, B. Onderka, K. Fitzner, *Bull. Acad. Sci. Polon. Ser. Techn.* **3**, 255 (1996).
- [16] M. Kopyto, K. Fitzner, *J. Solid State Chem.* **134**, 85 (1997).
- [17] M. Kopyto, K. Fitzner, *J. Solid State Chem.* **144**, 118 (1999).
- [18] B. Onderka, M. Kopyto, K. Fitzner, *J. Chem. Thermodyn.* **31**, 521 (1999).

- [19] G.G. Charette, S.N. Flengas, J. Electrochem. Soc. **115**, 796 (1968).
- [20] S.C. Schaefer, RI 8704, Bureau of Mines Report of Investigations, 1982, United States Department of the Interior.
- [21] V.A. Cherepanov, L. Yu. Barkhatova, A.N. Petrov, J. Phys. Chem. Solids **55**, 224 (1994).
- [22] T. Atsumi, T. Ohgushi, N. Kamegashira, J. Alloys and Comp. **238**, 35 (1996).
- [23] N. Kamegashira, Y. Miyazaki, Y. Hiyoshi, Mater. Chem. Phys. **10**, 299 (1984).
- [24] K.T. Jacob, Mrinalini Attaluri, K. Fitzner, Calphad J. **26**, (2002), in print.
- [25] H. Satoh, S. Suzuki, K. Yamamoto, N. Kamegashira, J. Alloys and Comp. **234**, 1 (1996).

REVIEWED BY: JAN WYPARTOWICZ

Received: 20 May 2002.